Pure & Appl. Chem., Vol. 48, pp. 407–414. Pergamon Press, 1976. Printed in Great Britain.

NEW EXPERIMENTAL AND THEORETICAL INVESTIGATIONS INTO KINETICS OF PHYSICAL ADSORPTION BY MICROPOROUS ADSORBENTS

M. M. DUBININ
Institute of Physical Chemistry, USSR Academy of Sciences, 117312 Moscow V-74, Leninskii pr. 31, USSR

Abstract—New experimental results on the kinetics of adsorption by microporous adsorbents are discussed. It is shown that the quasi-homogeneous model of a porous body is inapplicable for the description of the kinetics of adsorption by real microporous adsorbents.

New theoretical equations of the kinetics of adsorption by adsorbents with a biporous structure and their application for analysis of experimental data are considered.

1. INTRODUCTION

In accordance with the classification based on the mechanisms of adsorption and capillary phenomena occurring in adsorbent grains, their pores can be conveniently divided into micropores ($r < 6$–7 Å), supermicropores (6–$7 < r < 15$–16 Å), mesopores (15–$16 < r < 1000$–2000 Å), and macropores ($r > 1000$–2000 Å).[1,2] Here, r is the equivalent radius of the pore, which is equal to the ratio of the area of the normal cross-section of the pore to its perimeter.

In many cases of practical importance it is possible to simplify somewhat the real structure of the microporous adsorbents by isolating only two pore varieties widely differing in their properties, namely, adsorbing pores (micro- and supermicropores) and transport pores (meso- and macropores). This biporous structure of adsorbents can be represented by a simple model shown in Fig. 1. The hatched portions represent schematically the microporous zones of the adsorbent consisting exclusively of adsorbing pores. The space between the microporous zones represents transport pores.

The concepts of the biporous structure of microporous adsorbents were formulated as far back as the 1930's in Ref. (3). The scheme of the biporous structure of active carbons was also adopted in the work of Wicke.[4,5] As a rule, however, it was assumed that the rate of adsorption of a substance by the micropores is much higher than that of transfer within the transport pores. In later years the biporous, or bidisperse, structure was considered more or less comprehensively in a number of researches on adsorption[6–8] and catalysis.[9,10] At the same time, in quantitative consideration of the kinetics of physical adsorption the authors of most of the investigations proceeded from the quasi-homogeneous model of porous adsorbents. In this case the rate of mass transfer is characterized by effective diffusion coefficients, which are determined by solving the unsteady diffusion equation

$$\frac{\partial a}{\partial t} = D_e(\nabla^2 a) \tag{1}$$

where D_e is the effective diffusion coefficient, or the system of equations

$$\frac{\partial a}{\partial t} + \frac{\partial c}{\partial t} = \nabla(D_i \nabla c) \tag{2}$$

$$a = f(c) \tag{3}$$

with the corresponding initial and boundary conditions. Here, D_i is the internal diffusion coefficient, c and a are the local concentrations of the adsorbate in the gas and adsorption phases related by the adsorption isotherm eqn (3).

However, in studying real microporous adsorbents, for instance, zeolite pellets or microporous active carbons, this method of analysis of experimental data often leads to contradictory results. The limited applicability of the homogeneous model of a porous adsorbent is most often manifested in the dependence of the effective diffusion coefficient on the grain size of the adsorbent, which is devoid of any physical meaning. In a number of papers on adsorption kinetics (see, for instance Ref. 11) the authors point out the direct proportionality between some characteristic time to attain adsorption equilibrium t, and the adsorbent grain size, d, raised to a power of m. In this case the power index m varies from two (which corresponds to the homogeneous model of the adsorbent) to zero, when the characteristic adsorption time is independent of the adsorbent grain size. An analysis of extensive literature on the kinetics of adsorption by zeolite pellets, active carbons, and ion-exchange resins from the standpoint of the biporous structure of these adsorbents permits more rational interpretation of the experimental data in many cases.

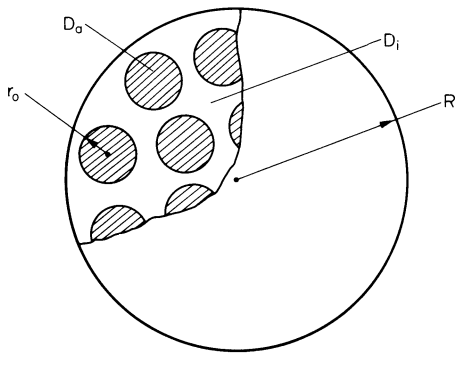

Fig. 1. Model of biporous adsorbent. R is radius of spherical grain of adsorbent, r_0 is radius of spherical microporous zones.

2. EXPERIMENT

Equations describing the macrokinetics of physical adsorption on adsorbents with a biporous structure have been obtained and analyzed in detail in Refs. 12–15. But before we consider the general equations of the kinetics of adsorption by biporous adsorbents and their application for quantitative analysis of experimental data, we wish to consider some experiments, whose objective was the qualitative analysis of the character of the mass transfer in real microporous adsorbents. Of great interest in studying the kinetics of adsorption of X-ray-contrast substances is the method of X-ray penetration of adsorbent granules.[15–17] An advantage of this method is the possibility of visual observation of the formation of the adsorption front and its propagation along the adsorbent grain. This permits the unambiguous determination of the limiting stage of internal diffusion mass transfer from the character of the adsorbate distribution in the adsorbent granule at successive time intervals.

Let us consider by way of example a granule of a zeolite pellet whose porous structure consists of adsorbing pores, i.e. micropores of zeolite crystals and spaces between the contacting crystals, which form the transport pores (Fig. 2). Now imagine a cylindrical granule of the adsorbent whose lateral surface is impermeable and where the adsorption of the X-ray-contrast substance occurs only from the end faces of the granule. It is obvious that if the adsorption rate is determined by diffusion in the zeolite crystals, the X-ray pictures will show gradual darkening of the entire adsorbent granule (Fig. 3a). If the process is limited by transfer in the transport pores, then for pronouncedly convex ("rectangular") adsorption isotherms we observe, as we know,[18,19] "layer-by-later" filling of the adsorbent granule (Fig. 3c). The intermediate case is characterized by the picture presented in Fig. 3b. This method was used in the present work in particular, to study the kinetics of adsorption of bromine- and iodine-containing hydrocarbons by *A*- and *X*- type zeolites.[16]

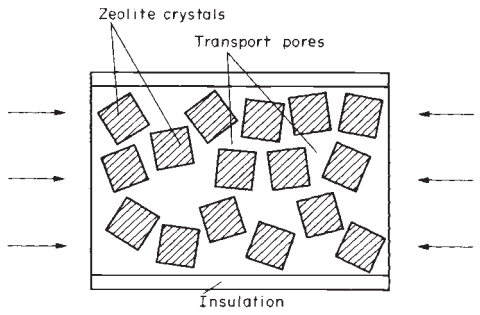

Fig. 2. Granule of zeolite pellet with impermeable lateral surface. Arrows indicate direction of adsorption flow.

When studying the character of transfer of the adsorbate in microporous active carbons by the X-ray technique, bromobenzene was used as an X-ray-contrast substance. We investigated the effect of the bromobenzene vapour pressure on the nature of the adsorbate transfer. The adsorbent, in the form of a cylindrical granule with an impermeable lateral surface, was fixed rigidly in an adsorption tube and photographed periodically under exposure to X-rays. The experiments were run at 298 K and at bromobenzene vapour pressures from 5 to 400 Pa (0.04–3 torr). Figure 4 exhibits X-ray pictures obtained in adsorption of bromobenzene by active carbons with molecular-sieve properties, MSC-5A.

The photographs (Fig. 4a) obtained at a relatively high adsorbtive pressure (400 Pa) show that the adsorption rate is determined by the transfer in the micropores (microporous zones) of the active carbon. With a decrease in pressure (27 Pa) the pattern of the process changed substantially (Fig. 4b). One can observe the formation of a considerably smeared-out adsorption front and its propagation along the grain. This indicates that the resistance to mass transfer in the adsorbing and transport pores is comparable. Finally, in adsorption from the carrier gas stream, the clear-cut picture of layer-by-layer filling of the adsorbent granule (Fig. 4c) points unambiguously to

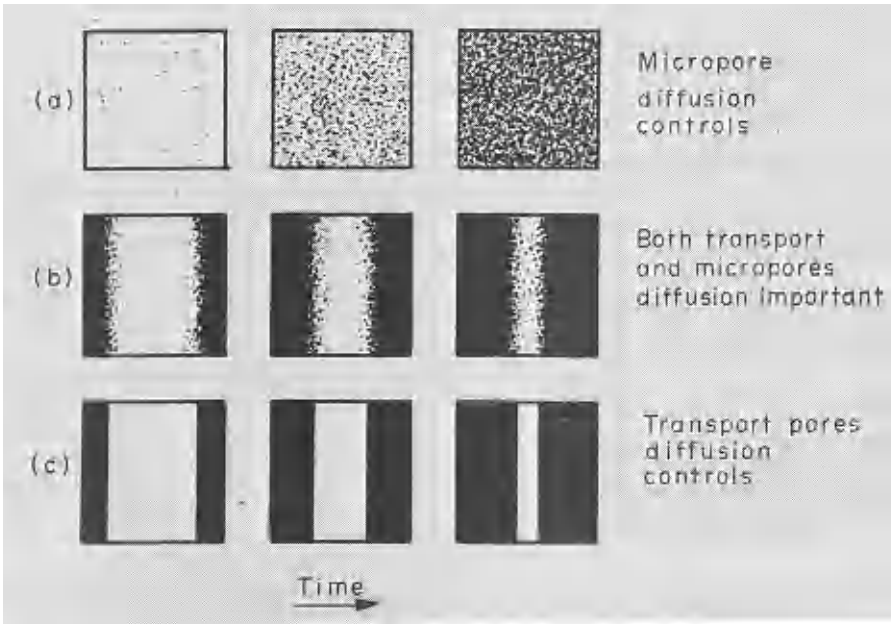

Fig. 3. Character of adsorbent distribution in granule of biporous adsorbent.

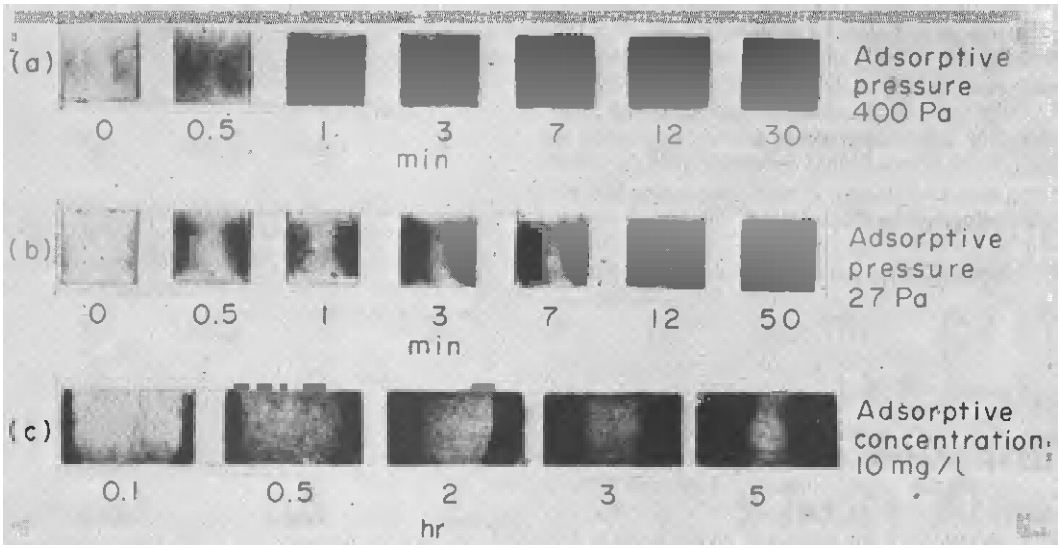

Fig. 4. Distribution of bromobenzene in granule of active carbon in successive time intervals.

the predominant role of the transfer in the transport pores.

The information necessary for a reliable qualitative analysis of experimental data on the kinetics of adsorption by adsorbents with a biporous structure can also be obtained in studying the rate of adsorption on grains of different sizes, or on granules of different geometrical shape, over a wide range of experimental conditions affecting the rate of transfer in adsorbing and transport pores.

Table 1 shows the results of experiments[20] which were conducted both on cylindrical granules of the adsorbent and on granules with an impermeable lateral surface. Such experiments permit estimation of the role of transfer in adsorbing and transport pores and of the applicability of the quasi-homogeneous model of a porous adsorbent for description of the adsorption kinetics. Table 1 contains only the qualitative inferences following from the analysis of the results obtained.[20]

According to Table 1 the variation in the character of the mass transfer with changes in adsorptive pressure and in adsorption from the carrier gas in the system benzene—MSC-5A and benzene—MSC-6A is similar to the one observed previously in the use of the X-ray technique (Fig. 4).

Thus an analysis of literature data and data obtained in the present work, as well as a study of the adsorption kinetics by the X-ray technique shows that the quasi-homogeneous model of a porous body is not applicable in the general case for description and interpretation of experimental data on the kinetics of adsorption by microporous adsorbents.

3. THEORY

Let us consider the model of biporous adsorbents which is represented schematically in Fig. 1. This model implies that microporous zones (for instance, small microporous crystals of zeolite in a granule) are randomly distributed throughout the granule, so that, on the average, N such crystals are contained in unit volume. It is also assumed that there are many microporous zones in the granule, so that it is possible to carry out the statistical averaging necessary for derivation of transfer macroequations. With these assumptions, we can isolate in a granule a physically infinitely small volume, $\Delta\Omega$, with macrocoordinates (x, y, z), which contains a sufficiently large

Table 1. Character of mass transfer of various substances in granules of microporous carbonaceous adsorbents

System	Adsorptive pressure, $P, Pa \times 10^{-3}$	Nature of transfer
Benzene–MSC-5A	0.21	Transfer in transport pores is the limiting stage
	7.78	Resistance to mass transfer in adsorbing and transport pores is comparable
Benzene–MSC-6A	0.21	Transfer in transport pores is the limiting stage
	7.78	Diffusion in micropores is the limiting stage
Benzene–MSC-5A, carrier gas Nitrogen	10 mg/l	Transfer in transport pores is the limiting stage
Water–MSC-5A	1.78	Diffusion in micropores is the limiting stage
Methanol-active carbon CK	0.28	Diffusion in micropores is the limiting stage
	0.40	Diffusion in micropores is the limiting stage
	0.54	Diffusion in micropores is the limiting stage
	0.69	Diffusion in micropores is the limiting stage

number of microporous zones but is small compared with the volume of the entire granule, $V \sim R^3$ (R is the determining size of the granule). The indicated condition is well fulfilled for real zeolite granules; for them, usually $(r_0/R) \sim 10^{-3}$ (r_0 is the characteristic size of the microporous zone). In connection with the above it is essential to emphasize that all the values appearing in the transfer macroequations for biporous adsorbents given below[13] are the respective average values for the indicated elementary volume.

The general adsorptive mass balance equation can be written as[13]

$$\frac{\partial a}{\partial t} + \frac{\partial c}{\partial t} = \nabla(D_i \nabla c), \quad a = a_1 + a_2. \tag{4}$$

Here, c, a are the concentrations of the adsorptive in the gas and adsorption phases averaged out over the physically infinitely small volume $\Delta\Omega$, D_i is the effective diffusion coefficient in the transport pores, a_1 and a_2 are the concentrations of the adsorbent on the walls of the transport pores and in the microporous zones.

In micropores, the division of the substance into parts in the free and adsorbed states loses its physical meaning.[1,2] Thus, in microporous zones the internal diffusion equation takes the form:

$$\frac{\partial a_*}{\partial t} = \frac{\partial}{\partial x_*}\left(D_a \frac{\partial a_*}{\partial x_*}\right) + \frac{\partial}{\partial y_*}\left(D_a \frac{\partial a_*}{\partial y_*}\right) + \frac{\partial}{\partial z_*}\left(D_a \frac{\partial a_*}{\partial z_*}\right) \tag{5}$$

where $a_1(\mathbf{r}, x*, y*, z*, t)$ is the local adsorptive concentration at the point (x_*, y_*, z_*) of the small crystal averaged over $\Delta\Omega$, D_a is the effective coefficient of diffusion in micropores.

Assuming, for simplicity, all microporous zones to be spheres of equal radius, r_0, we have, in addition to (4),[13]

$$\frac{\partial a_*}{\partial t} = \frac{1}{r_*^2}\left[\frac{\partial}{\partial r_*}\left(D_a r_*^2 \frac{\partial a_*}{\partial r_*}\right)\right],$$

$$a*(x, y, z, r_0, t) = f_2^*[c(x, y, z, t)],$$

$$\left[r_*^2\left(\frac{\partial a_*}{\partial r_*}\right)\right]_{r_*=0} = 0 \tag{6}$$

$$\frac{\partial a_2}{\partial t} = 4\pi r_0^2 N\left(D_a \frac{\partial a_*}{\partial r_*}\right)_{r_*=r_0},$$

$$a_1(x, y, z, t) = f_1[c(x, y, z, t)]. \tag{7}$$

Here, $f_1(c)$ and $f_2^*(c)$ are adsorption isotherms on the walls of the transport pores in microporous zones (averaged out over $\Delta\Omega$). The eqns (6) and (7) reflect the fact that the values a_* and a_1 on the external surface of the microporous zones (small crystals) and on the walls of the transport pores are related to c by the conditions of local equilibrium.

At D_a = const., eqns (4), (6), (7) can be reduced to the following

$$\frac{\partial a}{\partial t} + \frac{\partial c}{\partial t} = \nabla(D_i \nabla c),$$

$$\frac{\partial a}{\partial t} = \frac{\partial f_1(c)}{\partial t} + A\frac{\partial}{\partial t}\int_0^\theta f_2^*[c(x, y, z, \theta)]\psi(\theta - \sigma)\,\mathrm{d}\sigma \tag{8}$$

$$\psi(\theta) = 2\sum_{n=1}^{\infty} \exp(-\pi^2 n^2 \theta),$$

$$\theta = \frac{tD_a}{r_0^2}.$$

$$A = 4\pi r_0^3 N. \tag{9}$$

If the microporous zones have the shape of a cylinder with an impermeable lateral surface and a height of $2r_0$, or of a cylinder of radius r_0 with impermeable end faces, then, as is easily shown, eqns (8) retain their form, but ψ will be replaced, respectively, by

$$\psi_p(\theta) = \frac{2}{3}\sum_{n=1}^{\infty} \exp\left[-\frac{(2n-1)^2\pi^2\theta}{4}\right],$$

$$\psi_c(\theta) = \frac{4}{3}\sum_{n=1}^{\infty} \exp(-\rho_n^2\theta) \tag{10}$$

where ρ_n are the positive roots of a first-kind Bessel function of the zero order: $J_0(\rho_n) = 0$. These equations can be generalized for the case of arbitrary distribution of microporous zones by sizes.[21] In particular, if the adsorbent granule contains spherical zones of different radii, r_*, and $\chi(r_*)$ is the density function of the distribution of the microporous zones by radii, then the adsorption kinetics at constant D_a will be described by (4) and (11):

$$\frac{\partial a}{\partial t} = \frac{\partial f_1(c)}{\partial t} + 4\pi N\int_0^\infty r_*\chi(r_*)D_a \times\left\{\frac{\partial}{\partial t}\int_0^t f_2^*[c(x, y, z, \sigma)]\psi\left[\frac{D_a(t-\sigma)}{r_*^2}\right]\mathrm{d}\sigma\right\}\mathrm{d}r_*. \tag{11}$$

The above-considered equations cover only one internal diffusion resistance to the motion of the adsorbate molecule in a microporous zone, for instance in a small crystal of zeolite, and ignore the diffusion resistance to the entry of the molecule into the crystal associated with the overcoming of the potential barrier at the interface. There are indications[22] that this resistance may be considerable. Generalization of the main equations for this case was carried out in Ref. 23.

If the adsorption isotherms are nonlinear, only a numerical solution of the above equations is possible. For linear isotherms, $f_1(c) = k_1 c$, $f_2^*(c) = k_2^* c$, application of the statistical moments method permits the derivation of sufficiently simple analytical expressions relating D_a and D_i to the parameters of the adsorption isotherms and the moments of the kinetic curves, without the direct solution of these equations.

We will now determine the k-th order moment, M_k of the kinetic curve $\gamma(t)$ (γ is the relative adsorption value) as follows:

$$M_k = \int_0^\infty t^k\left(\frac{\mathrm{d}\gamma}{\mathrm{d}t}\right)\mathrm{d}t. \tag{12}$$

Calculation of M_k from the experimentally derived kinetic curve requires only the determination of the area of a figure bounded by the y-axis, the direct line $\gamma = 1$, and the kinetic curve in coordinates (γ, t^k) (Fig. 5). We have shown [24,25] that in the case of intradiffusion kinetics and linear adsorption isotherms, $f_1 = k_1 c$ and $f_2 = k_2^* c$, the

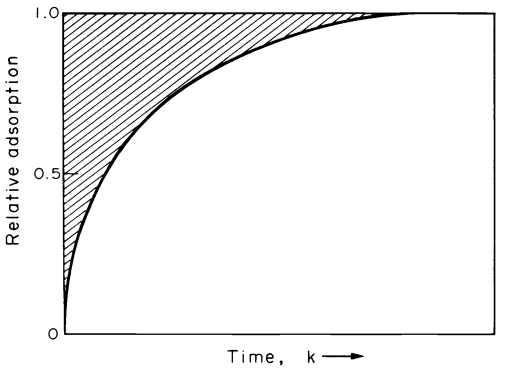

Fig. 5. Determination of statistical moments of experimental kinetic curves.

first-, second-, and third-order moments have the form

$$M_1 = g_{\nu 1}\tau_i + g_{\mu 1}B\tau_a,$$
$$M_2 = g_{\nu 2}\tau_i^2 + 4g_{\nu 1}g_{\mu 1}B\tau_i\tau_a + g_{\mu 2}B\tau_a^2,$$
$$M_3 = g_{\nu 3}\tau_i^3 + 9g_{\nu 2}g_{\mu 1}B\tau_i^2\tau_a + 6g_{\nu 1}(g_{\mu 1}^2 B + g_{\mu 2})B\tau_i\tau_a^2 + g_{\mu 3}B\tau_a^3. \quad (13)$$

Here, τ_a and τ_i are the characteristic times to adsorption equilibrium in the microporous zones and the transport porous system, and

$$\tau_i = \frac{L^2(1+\Gamma)}{D_i}, \quad \tau_a = \frac{r_0^2}{D_a}, \quad \Gamma = \frac{a_0}{c_0} = k_1 + \frac{Ak_2^*}{3},$$
$$B = \left[1 + \frac{3(1+k_1)}{Ak_2^*}\right]^{-1}. \quad (14)$$

L and r_0 are the determining dimensions of the granule and the microporous zones, respectively. If adsorption in the microporous zones is much greater than adsorption in the transport pores, which is usually the case for industrial adsorbents, then $B = 1$. The coefficient $g_{\nu 1}$, $g_{\nu 2}$, $g_{\nu 3}$ and $g_{\mu 1}$, $g_{\mu 2}$, $g_{\mu 3}$ depend, respectively, on the geometrical shape of the granule or the microporous zones; ν and μ ($\nu, \mu = 0, 1, 2$) are the shape indexes. The numerical values of these coefficients are determined from (15) and listed in Table 2.

$$g_{\nu 1} = [(\nu+1)(\nu+3)]^{-1},$$
$$g_{\nu 2} = 4[(\nu+1)^2(\nu+3)(\nu+5)]^{-1},$$
$$g_{\nu 3} = 6(5\nu+17)[(\nu+1)^3(\nu+3)^2(\nu+5)(\nu+7)]^{-1} \quad (15)$$

(the dependence of $g_{\mu i}$ on μ is evidently similar to that of $g_{\nu i}$ on ν (15)).

Table 2. Numerical values of shape coefficients

Shape of granule (microporous zone)	$\nu(\mu)$	$g_{\nu 1}$	$g_{\nu 2}$	$g_{\nu 3}$	β_ν
Cylinder with impermeable lateral surface (plate of thickness $2L$)	0	$\frac{1}{3}$	$\frac{4}{15}$	$\frac{34}{105}$	$\frac{1}{6}$
Cylinder of radius L with impermeable end faces	1	$\frac{1}{8}$	$\frac{1}{24}$	$\frac{11}{512}$	$\frac{1}{4}$
Sphere of radius L	2	$\frac{1}{15}$	$\frac{4}{315}$	$\frac{2}{525}$	$\frac{3}{10}$

If we calculate M_1 and M_2 from the experimental kinetic curve, as indicated above, and solve eqn (13) for the unknowns τ_i and τ_a, we can determine τ_i, τ_a and D_i. We can also calculate the first moments, M_1' and M_1'' for two adsorbent granules with identical internal structure but different size or shape.

The expressions for M_1 and M_2 have also been obtained for granules of cylindrical shape with an absolutely permeable external surface.[26] In this case

$$g_{\nu 1} = \frac{1}{8} - 4\mathscr{K}\sum_{n=1}^{\infty}\frac{th\left(\frac{\rho_n}{\mathscr{K}}\right)}{\rho_n^5},$$
$$g_{\nu 2} = \frac{1}{16} - 4\sum_{n=1}^{\infty}\frac{th^2\left(\frac{\rho_n}{\mathscr{K}}\right)}{\rho_n^6} - 12\mathscr{K}\sum_{n=1}^{\infty}\frac{th\left(\frac{\rho_n}{\mathscr{K}}\right)}{\rho_n^7} \quad (16)$$

where ρ_n are the roots of the Bessel function (see Ref. 10). Equations (13) and (16) make it possible to find expressions for M_1, M_2 for any $\mathscr{K} = (R/l)$ (R is the cylinder radius, $2l$ is its length) and are convenient enough, because the series in (16) converge rapidly.

The authors of Ref. 21 generalized the expressions for the moments M_1 and M_2 in the case of arbitrary size distribution of microporous zones in the granule. In this case the values τ_a and τ_a^2 in eqns (13) are determined by the equations

$$\tau_a = \overline{r_*^5}/D_a\overline{r_*^3}, \quad \tau_a^2 = \overline{r_*^7}/D_a^2\overline{r_*^3} \quad (17)$$

where

$$\overline{r_*^m} = \int_0^\infty r_*^m \chi(r_*)\,dr_*. \quad (18)$$

Consider now the case where adsorption occurs in a restricted volume, V_0, with an initial adsorptive concentration c_0. Under these conditions experiment has certain advantages. For the experimental kinetic curve we take the dependence

$$\gamma_V(t) = [c_0 - c(S,t)]/[c_0 - c_\infty]. \quad (19)$$

Here, $c(S,t)$ is the adsorptive concentration on the external surface of the granule, $c_\infty = c(S,\infty) = c_0/(1+\epsilon)$ is the equilibrium value of $c(S,t)$, $\epsilon = V(1+\Gamma)/V_0$, V is the granule volume. After calculating the moments M_{kv} for the curve $\gamma_V(t)$[27] we arrive at the following result

$$M_{1V} = (1+\epsilon)^{-1}(g_{\nu 1}\tau_i + g_{\mu 1}B\tau_a), \quad (20)$$
$$M_{2V} = (1+\epsilon)^{-2}\{g_{\nu 2}(1+\beta_\nu\epsilon)\tau_i^2 + 4g_{\nu 1}g_{\mu 1}B\tau_i\tau_a + [g_{\mu 2}(1+\epsilon) - 2\epsilon g_{\mu 1}^2 B]B\tau_a^2\} \quad (21)$$

where $\beta_\nu = 1 - (2g_{\nu 1}^2/g_{\nu 2})$ (see Table 2). As $V_0 \to \infty$ ($\epsilon \to 0$) eqns (20), (21) change to (13).

In studying the adsorption kinetics in a restricted volume, as well as in carrying out experiments at a constant adsorptive pressure (in order to calculate τ_i and τ_a) it is necessary to solve a system of two equations in two unknowns. For this, one must know either the first M_1 and the second M_2 moment of the kinetic curves or the first moments (M_1' and M_1'') for two adsorbent granules of different size or shape (see eqns (13)).

There is also another possibility for determining τ_i and τ_a, which does not require experiment with granules of

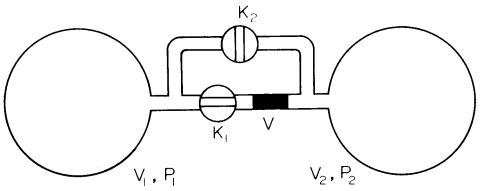

Fig. 6. Key diagram of experimental set-up for determining diffusion coefficients in adsorbing and transport pores during diffusion from one restricted volume into another.

different size or shape,[28] namely the study of the process of adsorptive diffusion from one restricted volume to another through the granule of the microporous adsorbent. The essence of this method is as follows. Let two volumes, V_1 and V_2, be separated by an adsorbent granule of volume V and length l (Fig. 6). Suppose at $t = 0$ the adsorptive concentration (or pressure) in the volume V_1 was equal to c_0 (or p_{01}), and the adsorbent and the volume V_2 were free from adsorptive. Then, in addition to eqns (8), we have the following boundary conditions

$$c_1(t) = c(x,t)|_{x=0} = c_0 + \frac{VD_i}{V_1 l}\int_0^t \left.\frac{\partial c}{\partial x}\right|_{x=0} dt \qquad (22)$$

$$c_2(t) = c(x,t)|_{x=l} = -\frac{VD_i}{V_2 l}\int_0^t \left.\frac{\partial c}{\partial x}\right|_{x=l} dt. \qquad (23)$$

Here, $c_1(t)$ and $c_2(t)$ are the adsorbate concentrations in the volumes V_1 and V_2 (we assume that the process of smoothing-out of concentration over the volumes V_1 and V_2 occurs much more rapidly than internal diffusion in the adsorbent). The kinetic curves will represent the dependences

$$\gamma_1(t) = [c_0 - c_1(t)]/[c_0 - c_\infty],$$
$$\gamma_2(t) = c_2(t)/c_\infty \qquad (24)$$

(c_∞ is the equilibrium adsorptive concentration in the system).

It can be shown that the first moments of these kinetic curves for the case of spherical microporous zones have the form

$$M_{11} = \frac{W_1}{(1+W_2)(1+W_1+W_2)}\left[\left(\frac{1}{3}+W_2+W_2^2\right)\tau_i + \frac{B}{15}\tau_a\right] \qquad (25)$$

$$M_{12} = \frac{1}{1+W_1+W_2}\left[\left(\frac{1}{6}+\frac{1}{2}W_1+\frac{1}{2}W_2+W_1W_2\right)\tau_i - \frac{B}{15}\tau_a\right] \qquad (26)$$

$$W_1 = \frac{V_1}{V(1+\Gamma)}, \quad W_2 = \frac{V_2}{V(1+\Gamma)}, \quad \tau_i = \frac{l^2(1+\Gamma)}{D_i}$$

from which:

$$\tau_i = \frac{2}{1+2W_2}\left(\frac{1+W_2}{W_1}M_{11} + M_{12}\right) \qquad (27)$$

$$\tau_a = \frac{30(1+W_2)}{BW_1(1+2W_2)}\left[\left(\frac{1}{6}+\frac{W_1+W_2}{2}+W_1W_2\right)M_{11} - \left(\frac{W_1}{3+3W_2}+W_1W_2\right)M_{12}\right]. \qquad (28)$$

At $W_2 = 0$ we get an equation similar to the one for adsorption from a finite volume (20)

$$M_{22} = \frac{W_1}{1+W_1}\left(\frac{1}{3}\tau_i + \frac{B}{15}\tau_a\right). \qquad (29)$$

If the adsorption of the diffusing gas can be neglected ($W_{1,2} \gg 1$)

$$M_{11} = M_{12} = M_1 = \frac{W_1W_2}{W_1+W_2}\tau_i; \quad \tau_i = M_1\left(\frac{1}{W_1}+\frac{1}{W_2}\right). \qquad (30)$$

Thus, by calculating M_{11} and M_{12} from the experimental curves $\gamma_1(t)$ and $\gamma_2(t)$, we can determine τ_i and τ_a by solving eqns (27) and (28).

The curves $c_1(t)$ and $c_2(t)$ (and, respectively, $\gamma_1(t)$ and $\gamma_2(t)$) may have the form shown in Fig. 2, depending on the ratio between τ_i and τ_a. At $W_{1,2} \gg 1$ (i.e. the change in the adsorbate concentration in the system due to adsorption is negligibly small) the dependence $c_2(t)$ has the form given in Fig. 7(2a). An experiment run under these conditions is similar to an experimental study of adsorbent permeability for nonsorbing gases. If τ_i is sufficiently small compared to τ_a, the adsorptive may initially quickly penetrate from the volume V_1 into the volume V_2 through the transport pores of the adsorbent and only then be finally adsorbed by the micropores (Fig. 7(2c)). Here, the curve $\gamma_2(t)$ will have a portion $\gamma_2 > 1$ and the area above the straight line $\gamma = 1$ must be assumed negative. In the limiting case $\tau_a \gg \tau_i$ the experiment is similar to the study of the kinetics of adsorption from a restricted volume (Fig. 7(2d)).

In previously published works on adsorption dynamics it was assumed that the adsorbent grains have uniform pores, and the internal diffusion in them was characterized by a single diffusion coefficient. At the same time, it can be seen from the foregoing that the porous structure of zeolite pellets and active carbons can be interpreted more correctly as a bidisperse one which can manifest itself prominently in the course of adsorption. Natural porous and granular media, including particles of soils and rocks, also have a porous structure of the indicated type. In this connection it is expedient to investigate the adsorption dynamics in a layer of grains with a bidisperse porous structure. This investigation was carried out in Ref. 29.

4. DISCUSSION

The use of the obtained equations for calculating τ_i and τ_a can be considered for the case of analysis of

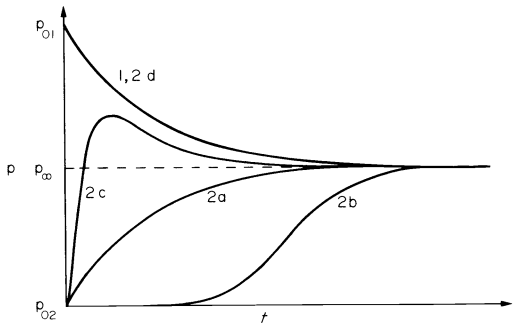

Fig. 7. Character of curves $p_1(t)(1)$ and $p_2(t)(2)$ in diffusion of adsorptive from one volume into another through adsorbent granule.

experimental data on the kinetics of adsorption of *n*-pentane by the Czechoslovak active carbon Supersorbon.[20] The study of adsorption kinetics was conducted on three adsorbent fractions of different grain size composition in the pressure range from 3 to 3×10^4 Pa. All the fractions of the active carbon with equivalent particle radii of 1.75, 0.68 and 0.10 mm and practically identical adsorption isotherms were obtained by grinding the initial adsorbent fraction with subsequent sieving. Measurements were made for all the fractions simultaneously in three adsorption tubes of a gravimetric installation at a constant pressure of *n*-pentane vapours. The adsorption kinetics were studied with a stepwise variation in adsorptive pressure in the adsorption set-up, thus enabling us to apply the corresponding adsorption kinetics equations for linear isotherms to the experimental data obtained.

The dependences of the effective diffusions coefficients, D_e, on the adsorptive vapour pressure presented in Fig. 8 were obtained by treatment of experimental data with the use of equations for the quasi-homogeneous adsorbent model. It can be seen that the effective diffusion coefficients thus determined from experimental data for grains of different size may differ by several orders. Besides, in one case D_e varies uniformly with increasing pressure (Fig. 8c), while in another (Fig. 8a) this dependence is of an extremal nature.

Let us now analyze the presented experimental data with the aid of expressions obtained in the theoretical part. The treatment of experimental data by means of equations for biporous adsorbents enables one to calculate the effective coefficient of diffusion in the transport pores, D_e, and the effective diffusion parameter D_a/r_0^2 and to explain the results obtained by the traditional method of analysis. The dependences of D_e and D_a/r_0^2 on the adsorptive pressure are shown in Fig. 9. An increase in D_e with the pressure (with simultaneous decrease in D_a/r_0^2) explains the shape of the dependence of D_e on the pressure in Fig. 8a. At low adsorptive pressures we will notice, for this grain fraction, the contribution from the resistance to mass transfer in the transport pores, and therefore with an increase in pressure one observes some increase in D_e (corresponding to the increase in D_e in Fig. 8). With increasing pressure, diffusion in the adsorbing pores becomes the

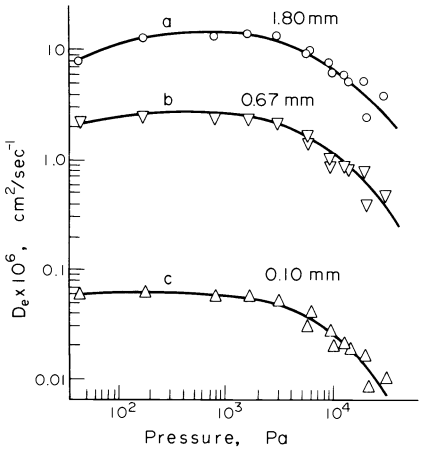

Fig. 8. Dependence of effective diffusion coefficient on pressure of *n*-pentane for three fractions of active carbon. R = 1.8 mm, 0.67 mm and 0.10 mm.

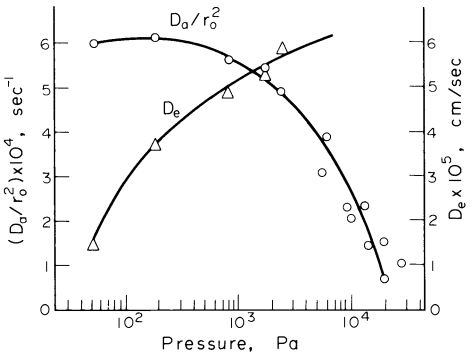

Fig. 9. Dependence of effective coefficient of diffusion in transport pores, D_e, and effective diffusion parameter for micropores, D_a/r_0^2 on adsorptive pressure in system *n*-pentane–Supersorbon.

controlling stage of mass transfer and the decrease in D_e with pressure in Fig. 8 reflects the pressure dependence of D_a/r_0^2 in Fig. 9. The obtained results agree with those of the studies into the kinetics of adsorption of benzene by active carbons MSC-5A and MSC-6A and of bromobenzene by active carbon MSC-5A using the X-ray technique.

The application of the method of investigation to diffusion from one restricted volume into another for calculation of τ_i and τ_a can be illustrated by considering the diffusion of xenon through a granule of microporous active carbon MSC-5A at temperatures of 195 and 300 K. The key diagram of the set-up is given in Fig. 6. Xenon passes from volume V_1 (initial pressure p_{01}) to volume V_2 (initial pressure p_{02}) until equilibrium pressure, p_∞, is established. The curves $p_1(t)$ and $p_2(t)$, which are similar to those presented in Fig. 7 (1, 2a) were obtained, for instance, under the following experimental conditions: T = 195 K, p_{01} = 1 kPa, p_{02} = 0, p_∞ = 0.2 kPa, V_1 = 395 cm³, V_2 = 118 cm³, $\Gamma = 2.5 \times 10^4$, $L = 2R$ = 0.42 cm. At higher average adsorptive pressures in the set-up (Γ is small and $W_{1,2} \gg 1$), and also at an experimental temperature of 3000 K, the curves $p_2(t)$ have the form shown in Fig. 7(2b). In this case the value of τ_i was calculated by eqn (30). The experimental results are depicted in Fig. 10. It can be seen that the diffusion coefficients calculated by eqn (27), with an allowance for adsorption, fall on a straight line extrapolated from the high-pressure range, where coefficient Γ is negligibly small, and τ_i is calculated by eqn (30). The results obtained are also in good agreement with the

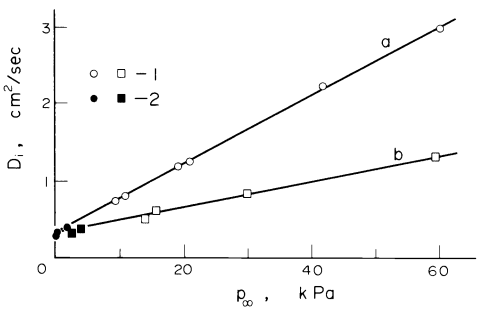

Fig. 10. Dependence of coefficient of diffusion of xenon in transport pores of active carbon MSC-5A on adsorptive pressure at temperature of 195 K (a) and 300 K (b) 1. Calculation of D_i by eqn (30); 2. Calculation of D_i by eqn (27) with allowance for adsorption.

results of the study into the kinetics of adsorption from a restricted volume for the same system.

Thus, by using one or other of the experimental methods available for studying the kinetics of adsorption by porous adsorbents and the relevant expressions for analysis of the experimental data obtained, we can analyze the effect of the experimental conditions on the transfer rate in the adsorbing and transport pores and determine the contribution from each type of transfer to the total adsorption rate. This enables us to approach more efficiently the choice of adsorbents with the most rational porous structure. In addition, knowledge of the rate-determining stage of the adsorption kinetics will enable recommendation of an approximate adsorption-kinetics equation for solving problems of adsorption dynamics, which is physically justified.

In this work, we used mainly the results obtained by researchers of the Institute of Physical Chemistry of the USSR Academy of Sciences I. T. Erashko, V. I. Ulin, A. M. Voloshchuk and P. P. Zolotarev under the guidance of M. M. Dubinin, and the results of O. Kadlec's investigations carried out at the Institute of Physical Chemistry and Electrochemistry of the Czechoslovak Academy of Sciences.

REFERENCES

[1]M. M. Dubinin, *Adv. Colloid Interface Sci.* **2**, 217 (1968).
[2]M. M. Dubinin, *Prog. Surface Membrane Sci.* **9**, 1 (1975).
[3]M. M. Dubinin, *Fiziko-khimicheskie Osnovy Sorbtsionnoi Tekhniki.* Goskhimtekhizdat, Moscow (1932).
[4]E. Wicke, *Kolloid Z.* **86**, 167 (1939).
[5]E. Wicke, *Kolloid Z.* **93**, 129 (1940).
[6]P. K. C. Wiggs, *Conf. Industrial Carbon*, London (1957).
[7]D. P. Timofeev and I. T. Erashko, *Dokl. Akad. Nauk SSSR* **132**, 144 (1960).
[8]D. P. Timofeev, *Adv. Chem. Ser.* **102**, 247 (1971).
[9]N. Wakao and J. M. Smith, *Chem. Eng. Sci.* **17**, 825 (1962).
[10]P. Montarnal, v sbornike *Poristaja Struktura Katalizatorov i Protsessy Perenosa v Geterogennom Katalize.* Vol. 93, Nauka, Novosibirsk (1970).
[11]L. A. Kovalenko, Yu. I. Shumjatskiy and N. V. Keltsev, *Teor. osnovy khim. tekhnol.* **2**, 869 (1968).
[12]E. Ruckenstein, A. S. Vaidyanathan and G. R. Youngquist, *Chem. Eng. Sci.* **26**, 1305 (1971).
[13]P. P. Zolotarev and M. M. Dubinin, *Dokl. Akad. Nauk SSSR* **210**, 1136 (1973).
[14]A. M. Voloshchuk, M. M. Dubinin and P. P. Zolotarev, 4 *Vsesojuznaja Konferentsija po teoreticheskim voprosam adsorbtsii.* Rasshirennye tezisy dokladov, Vyp. 2, s. 72, Nauka, Moscow (1973).
[15]M. Kochirzhik and A. Zikanova, 4 *Vsesojuznaja Konferentsija po teoreticheskim voprosam adsorbtsii.* Rasshirennye tezisy dokladov, Vyp. 2, s. 88, Nauka, Moscow (1973).
[16]A. M. Voloshchuk and M. M. Dubinin, *Dokl. Akad. Nauk SSSR* **212**, 649 (1973).
[17]A. M. Voloshchuk, M. M. Dubinin and I. T. Erashko, *Izvest. Akad. Nauk SSSR, Ser. Khim.* 1931, 1937 (1974).
[18]D. P. Timofeev, *Zh. Fiz. Khim.* **39**, 2735 (1965).
[19]D. P. Timofeev and A. A. Voskresenskii, *Dokl. Akad. Nauk SSSR* **122**, 434 (1958).
[20]I. T. Erashko, O. Kadlec, A. M. Voloshchuk and M. M. Dubinin, *Izvest. Akad. Nauk SSSR, Ser. Khim.* 1937 (1974).
[21]P. P. Zolotarev and V. I. Ulin, *Izvest. Akad. Nauk SSSR, Ser. Khim.* 1648 (1974).
[22]J. Karger and J. Caro, *J. Colloid Interface Sci.* **52**, 623 (1975).
[23]P. P. Zolotarev, *Izvest. Akad. Nauk SSSR, Ser. Khim.* 193 (1975).
[24]A. M. Voloshchuk, P. P. Zolotarev and V. I. Ulin, *Izvest. Akad. Nauk SSSR, Ser. Khim.* 1250 (1974).
[25]V. I. Ulin, *Izvest. Akad. Nauk SSSR, Ser. Khim.* 1653 (1974).
[26]V. I. Ulin, *Izvest. Akad. Nauk SSSR, Ser. Khim.* 2148 (1974).
[27]P. P. Zolotarev and V. I. Ulin, *Izvest. Akad. Nauk SSSR, Ser. Khim.* 2829 (1974).
[28]A. M. Voloshchuk, M. M. Dubinin, N. A. Nechaeva and V. I. Ulin, *Dokl. Akad. Nauk SSSR* **223**, 2, 369 (1975).
[29]P. P. Zolotarev and V. I. Ulin, *Izvest. Akad. Nauk SSSR, Ser. Khim.* 2858 (1974).